Quaternary Science Reviews 55 (2012) 23–33

Contents lists available at SciVerse ScienceDirect

Quaternary Science Reviews

journal homepage: www.elsevier.com/locate/quascirev

Invited paper

A re-examination of evidence for the North Atlantic "1500-year cycle" at Site 609

Stephen P. Obrochta [a,*], Hiroko Miyahara [b], Yusuke Yokoyama [c], Thomas J. Crowley [d]

[a] University of Tokyo Atmosphere Ocean Research Institute, Kashiwa, Chiba 227-8564, Japan
[b] University of Tokyo Institute for Cosmic Ray Research, Japan Agency for Marine-Earth Science and Technology, Japan
[c] University of Tokyo Atmosphere Ocean Research Institute, University of Tokyo Department of Earth and Planetary Sciences, Japan Agency for Marine-Earth Science and Technology, Japan
[d] Braeheads Institute, Maryfield, Braeheads, East Linton, East Lothian, Scotland EH40 3DH, UK

ARTICLE INFO

Article history:
Received 27 March 2012
Received in revised form
7 August 2012
Accepted 13 August 2012
Available online

Keywords:
North Atlantic
Paleoceanography
Ice-rafted debris (IRD)
Stratigraphy
Millennial climate variability
Solar variability

ABSTRACT

Ice-rafting evidence for a "1500-year cycle" sparked considerable debate on millennial-scale climate change and the role of solar variability. Here, we reinterpret the last 70,000 years of the subpolar North Atlantic record, focusing on classic DSDP Site 609, in the context of newly available raw data, the latest radiocarbon calibration (Marine09) and ice core chronology (GICC05), and a wider range of statistical methodologies. A ~1500-year oscillation is primarily limited to the short glacial Stage 4, the age of which is derived solely from an ice flow model (ss09sea), subject to uncertainty, and offset most from the original chronology. Results from the most well-dated, younger interval suggest that the original 1500 ± 500 year cycle may actually be an admixture of the ~1000 and ~2000 cycles that are observed within the Holocene at multiple locations. In Holocene sections these variations are coherent with ^{14}C and ^{10}Be estimates of solar variability. Our new results suggest that the "1500-year cycle" may be a transient phenomenon whose origin could be due, for example, to ice sheet boundary conditions for the interval in which it is observed. We therefore question whether it is necessary to invoke such exotic explanations as heterodyne frequencies or combination tones to explain a phenomenon of such fleeting occurrence that is potentially an artifact of arithmetic averaging.

1. Introduction

The late Gerard Bond and colleagues reported from multiple locations across the North Atlantic a "1500-year cycle" in ice-rafted, hematite-stained grains (HSG) that appeared to pace the Dansgaard–Oeschger (D–O) Events prominent in the last-glacial interval of the GISP2 Greenland ice core (Bond and Lotti, 1995; Bond et al., 1997, 1999). The subsequent interpretation of solar forcing of HSG variability during the Holocene (Bond et al., 2001) stimulated substantial debate on the mechanisms of millennial variability, due in part to the lack of a corresponding 1500-year solar cycle. This body of work remains widely discussed, with the above-mentioned four manuscripts being cumulatively cited in excess of 3000 times.

Classic DSDP Site 609 (49° 52.7′ N, 24° 14.3′ W; 3884 mbsl), located on the upper–middle eastern flank of the Mid Atlantic Ridge within the "IRD Belt" of Ruddiman (1977), produced one of the more well-known HSG records (Fig. 1). In addition, this site was instrumental in linking Greenland air temperature with North Atlantic sea surface temperature (SST) fluctuations, as well as in demonstrating that D–O Events are bundled into progressively cooler interstadials that culminate in a large ice discharge (Heinrich Event) (Bond et al., 1992, 1993).

During IODP Exp. 303, Site 609 was reoccupied, and a continuous 355 m sequence was recovered from Site U1308 (Exp. 303 Scientists, 2006). Hodell et al. (2008) used grayscale variations to correlate the two sites, allowing for the transfer of the Site 609 age model to Site U1308. However, the utility of the Site 609 age model is currently limited due to its basis in older chronologies that have since undergone significant revision.

Therefore, in this manuscript we reinterpret the HSG record of DSDP Site 609 (Bond et al., 1999) in light of an improved chronology for the last glaciation, Marine Isotope Stages (MISs) 2–4. We 1) reassess the chronostratigraphic correlation between Site 609 and the Greenland ice core record, 2) improve the early-glacial chronology with the virtually complete North GRIP (NGRIP) ice core (NGRIP Project Members, 2004), and 3) temporally extend the late-glacial radiocarbon chronology with the most recent marine radiocarbon calibration curve (Reimer et al., 2009). We then 4) apply an age uncertainty model to this thoroughly updated chronology to evaluate the effects of age perturbations on cyclicity.

* Corresponding author.
E-mail address: obrochta@aori.u-tokyo.ac.jp (S.P. Obrochta).

0277-3791/$ – see front matter
http://dx.doi.org/10.1016/j.quascirev.2012.08.008

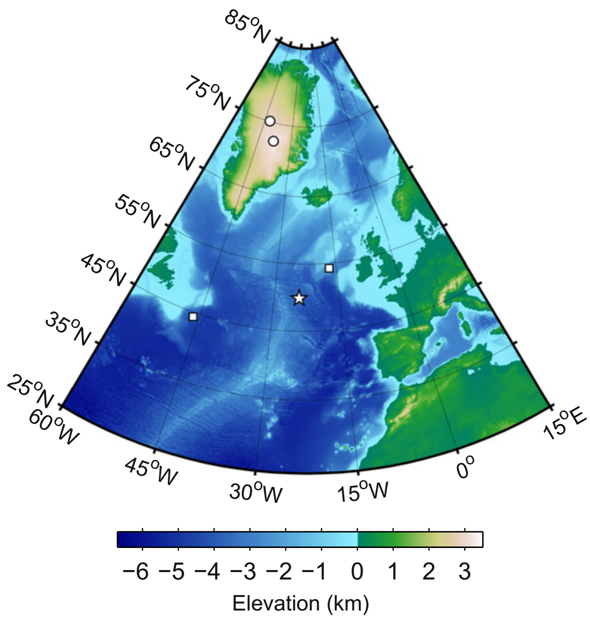

Fig. 1. Star depicts the location of Site 609 (49°52.7′N, 24°14.3′W; 3884 mbsl). Squares represent locations of western and eastern cores, MC21 and GGC22 (44°18′N, 46°16′W; 3958 mbsl), MC52 (55°28′N, 14°43′W, 2172 mbsl), V29-191 (54°16′N, 16°47′W, 2370 mbsl), and V23-81 (54°15′N, 16°50′W, 2393 mbsl). Circles denote Greenland ice cores GISP2 (72°36′N, 38°30′W; 3200 m) and NGRIP (75°6′N, 42°20′W; 2917 m).

Finally, we 5) make available the entire Site 609 dataset (see Supplemental Online Material) with the goal of enabling better global correlation to this important location.

2. Background

2.1. Sources and significance of hematite stained grains

Over forty years ago, Paleozoic red beds in the area of the Gulf of St. Lawrence, which contain abundant hematite-cemented quartz sandstones (e.g., Belt, 1965), were proposed as a primary source for ferruginous sediments transported to the North Atlantic basin during Pleistocene glaciations (Heezen et al., 1966). Ericson et al. (1961) first described these sediments in western North Atlantic sediment cores during the early days of the Lamont-Doherty Earth Observatory's "core a day" program. Subsequently, similar sediments were discovered at the mouth of the Gulf of St. Lawrence (Heezen and Drake, 1964) and in Baffin Bay (Marlowe, 1968). The latter, however, does not appear to significantly export ferruginous sediment because of the lack of such deposits in the Labrador Sea (Hollister, 1967). Pollen (Needham et al., 1969) and clay mineral (Conolly et al., 1967; Zimmerman, 1972) assemblages also strongly suggest a Gulf of St. Lawrence source.

Sediment cores taken along major iceberg trajectories later corroborated the interpretation that ice-rafted HSG were primarily derived from the Gulf of St. Lawrence during the last glaciation (Bond and Lotti, 1995). During the Holocene, however, core top analyses indicate other sources for HSG. Red beds from East Greenland and Svalbard, and likely the Arctic Ocean, contributed significant amounts of HSG, and changes in ocean circulation (as opposed to increased calving) are interpreted to be responsible for variations in the amount of HSG deposited in the modern subpolar North Atlantic (Bond et al., 1997). Thus, Bond et al. (1997) concluded that HSG deposition from melting ice is controlled by differing mechanisms during the Holocene and long interstadials (ocean circulation changes) and during glacial times (increased iceberg discharge).

2.2. HSG methodology

Bond and Lotti (1995), as well as Bond et al. (1997, 1999, 2001), performed counts of HSG, detrital carbonate (DC), and Icelandic glass (IG) on the 63–150 μm size fraction using grain-mount slides and a petrographic microscope. This size fraction was chosen to provide "greater accuracy in petrologic identification" (Bond and Lotti, 1995). Using a narrow range of relatively small-sized grains also reduces variability resulting from any relationship between grain size and composition (Bond et al., 1999) without introducing a compositional bias (Bond and Lotti, 1995). Grain-mount slides allow multiple grain faces to be viewed at once, increasing identification efficiency. In addition, the relative abundance of the 63–150 μm fraction remains high during interglacials, allowing standardized measurements from both interglacial and glacial times (Bond et al., 1999). Counts of bulk lithic grains and *Neogloboquadrina pachyderma* (s) were performed on the >150 μm fraction using standard techniques (Bond and Lotti, 1995; Bond et al., 1997).

2.3. Principal HSG results

Early discussion of HSG focused on its potential for integrating much of the observed last-glacial millennial variability. Grootes and Stuvier (1997) identified a sharp, highly significant 1470-year spectral peak in the Greenland GISP2 ice core $\delta^{18}O$ record. Coincidentally, Bond et al. (1997) reported a mean pacing of 1470 ± 523 years in HSG deposition. Peaks in HSG deposition occurred simultaneously with increases in IG and preceded each of the large "Hudson Strait" Heinrich Events (H1, H2, H4, H5), which are recognizable by abrupt increases in DC (Bond and Lotti, 1995; Bond et al., 1999). Therefore, the 1500-year cycle in HSG potentially explained not only the pacing of the D–O Events evident in Greenland ice cores (e.g., Schulz, 2002; Rahmstorf, 2003) but also offered an explanation for surging of the Laurentide Ice Sheet (LIS): climate acting on unstable ice in multiple locations that simultaneously surges and in turn destabilizes the LIS, perhaps due to the effects of sea level rise on grounded ice margins, producing a Heinrich Event.

However, neither the last glacial nor Holocene HSG records exhibit statistically significant 1500-year periodicity. Therefore these records were referred to as either "quasi-periodic" (Bond et al., 1997) or "cyclic" (in a geologic sense, implying repetition, not periodicity) (Bond et al., 2001). The mean pacing of 1470 ± 523 years was derived by interval counting (the elapsed time between cycle midpoints) and was the combined result of a composite record covering the last glaciation with V23-81 (1536 ± 563 years) and the Holocene with V29-191 (1374 ± 502 years) (Bond et al., 1997). Bond et al. (1999) later revised the V23-81 result to 1469 ± 514 years and presented results for the last glacial interval of DSDP Site 609 (1476 ± 585 years).

The most well-known HSG record is the eastern (MC21-GGC22) and western (MC52-V29-191) North Atlantic Holocene stack that was shown to be highly coherent with cosmogenic nuclide production. While this was used to suggest that "at least the Holocene segment of the North Atlantic's '1500-year' cycle appears to have been linked to variations in solar irradiance" (Bond et al., 2001), the coherency was, in fact, not at 1500 years at all but at primarily 500, 1000, and perhaps 2000 years. (Variability at the latter period was filtered out of the records prior to cross-spectral analysis.) The absence of coherency at a ∼1500-year period reflects the lack of power at this band in the HSG and solar proxy records. Variations in this stacked record coincided with well-known climatic events, including the 8.2 ka Event, Medieval Warm Climate Anomaly, and Little Ice Age, (Bond et al., 1997, 2001), but these climate events are not spaced at 1500-year intervals. The phrase "1500-year," as it appears in Bond et al. (2001), is a generic descriptor that, in every instance, may be replaced with "HSG"; it does not indicate that there is coherence with solar variability at a 1500-year period.

Applying the results of Bond et al. (2001) to the last-glacial HSG records presents a conundrum. Either the solar forcing would require modification, e.g., heterodynes (Clemens, 2005) and combination tones (Braun et al., 2005) of centennial scale oscillations, or the ~1500 ± 500-year cycle is more consistent with ~1000- and perhaps ~2000-year variability. Indeed, subsequent work reduced the importance of an exact 1470-year mean HSG cycle length by demonstrating that the 1470-year spectral peak results from three extremely regularly spaced D–O warming events in GISP2 (Schulz, 2002) and is absent from other Greenland ice cores (e.g., Clemens, 2005; Ditlevsen et al., 2007).

3. Methods

3.1. Age model

We update the radiometrically-dated portion of the Site 609 age model to reflect recent improvements to the last glacial chronology provided by the Marine09 radiocarbon calibration (Reimer et al., 2009). Though the radiocarbon dating of Site 609 extends into MIS 3, the original chronology was based on only dates up to 19,340 ^{14}C years that were converted to calendar ages using the calibration of Bard et al. (1993) and resulted in a maximum calendar age of 22,646 years BP (BP is relative to 1950 AD). Here, we use Calib 6.0 (Stuiver and Reimer, 1993) to recalculate new calendar ages and include eleven previously uncalibrated dates, extending the radiocarbon-dated interval of this site to 31,120 ^{14}C years BP (Table 1). A constant global reservoir correction (405 years) is applied by the Calib program. We do not specify a local reservoir correction (ΔR). All radiocarbon dates were performed on planktic foraminifers, none of which were sampled from Heinrich layers. This greatly reduces the possibility of large reservoir age changes associated with fluctuations in thermohaline circulation and of contamination from infilling with radiocarbon-dead, fine-grained detrital carbonate (Hodell and Curtis, 2008).

From early MIS 3, beyond the radiocarbon-dated interval, Bond et al. (1999) exported the Meese/Sowers (M/S94) GISP2 ice core chronology to Site 609 by tying the % *N pachyderma* (s) SST proxy record to the GISP2 ice core (Fig. 2), which is layer counted to 55 ka (Bender et al., 1994; Meese et al., 1997). However, very high density sampling of the new, virtually complete North GRIP (NGRIP) ice core indicates that GISP2 likely suffers from excessive layer thinning (Svensson et al., 2006). Therefore, we improve the older portion of the Site 609 age model by aligning the SST proxy and the NGRIP δ^{18}O records, allowing us to import the latest Greenland ice core chronology (GICC05, layer counted to 60 ka beyond which the ss09sea flow model is applied) (Svensson et al., 2008). We rely on the original Site 609 depth tie points of Bond et al. (1999) (Table 2), which are primarily lows in *N. pachyderma* (s) abundance. These are correlated to the corresponding events in the NGRIP ice core (e.g, peak low percent tied to peak interstadial δ^{18}O) (Fig. 2). This procedure assumes North Atlantic sea surface and Greenland air temperature variations are in phase. Supplemental Fig. 1 compares each ice core record to the Site 609 *N. pachyderma* (s) record in down-core depth.

3.2. Spectral analysis

In a similar fashion as Bond et al. (1997, 1999), we calculate the elapsed time between cycle midpoints. Multitaper method (MTM) spectral analysis is performed using the software package SSA-MTM Toolkit (Ghil et al., 2002) after interpolating to a 200-year time step, which is a slightly lower resolution than the average sampling resolution of ~180 years. Morlet wavelet analysis is performed using Matlab with code available for download at http://paos.colorado.edu/research/wavelets/software.html (Torrence and Compo, 1998). Prior to wavelet analysis, the data were first detrended and smoothed by subtracting the first SSA-reconstructed (trend) component before interpolation to a 200-year interval and application of a 500-year lowpass filter.

3.3. Age uncertainty model

Alternate age models are calculated by allowing the age control points of Site 609 to vary independently within their respective Gaussian 2σ ranges to assess the robustness of HSG variability to plausible chronological perturbations. Because there is no published uncertainty for the ss09sea flow model that was used to assign ages in excess of 60 ka to NGRIP, the corresponding interval of Site 609 is excluded. For radiocarbon dates, the 2σ range in calibrated calendar years is used. NGRIP-derived dates use the

Table 1
Site 609 radiocarbon dates.

Depth (cm)	^{14}C years (uncorrected)	σ (y)	Original calibration (y BP 1950)	Marine09 calibration (y BP 1950)	1σ range (BP 1950)	2σ range (y BP 1950)
55	11,500	–	–	12,980	12,860–13,120	12,700–13,190
73.5	12,750	220	14,474	14,440	14,020–14,690	13,800–15,140
79.5	13,650	90	15,590	16,190	15,910–16,600	15,430–16,750
84.5	14,990	230	17,252	17,740	17,400–18,030	17,120–18,160
87.5	16,360	240	18,950	19,120	18,920–19,380	18,660–19,480
90.5	16,760	150	19,446	19,510	19,390–19,600	19,210–19,930
98.5	17,360	120	20,190	20,130	19,970–20,320	19,810–20,420
107.5	19,340	220	22,646	22,610	22,280–22,720	22,120–23,340
110.5	20,370	330	–	23,850	23,470–24,270	22,930–24,570
111.5	20,950	260	–	24,530	24,250–24,910	23,850–25,120
112.5	21,510	220	–	25,230	24,910–25,590	24,540–25,870
115.5	21,770	220	–	25,540	25,190–25,850	24,960–26,160
118.5	22,780	340	–	27,000	26,600–27,640	26,050–27,920
140.5	25,660	440	–	30,050	29,580–30,430	29,300–30,970
148.5	26,570	310	–	30,840	30,630–31,090	30,360–31,220
153.5	29,570	660	–	33,670	33,070–34,580	31,930–34,900
166.5	30,480	680	–	34,640	33,640–35,220	33,150–36,310
174.5	31,120	730	–	35,360	34,690–35,660	33,700–36,670

^{14}C dates are uncorrected for reservoir age and from Bond et al. (1993). The date at 55 cm is from Elliot et al. (1998), and does not include a reported error; we assumed a value of 100 years. Marine09 calibration is from (Reimer et al., 2009). The reported calibration ages are the rounded, median probability determined by the online version of Calib 6.0 (Stuiver and Reimer, 1993).

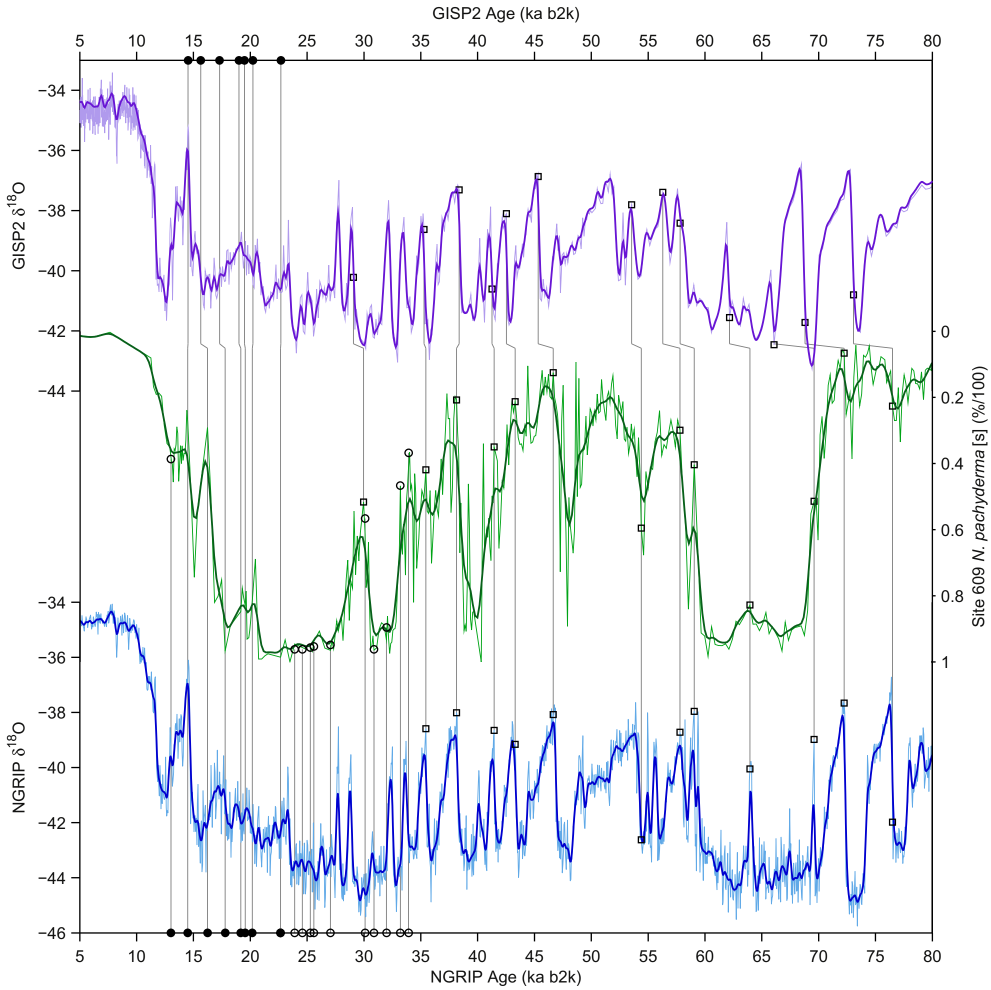

Fig. 2. The GISP2 ice core $\delta^{18}O$ record (purple, top) is tied to the Site 609% *N. pachyderma* (s) record (green, middle) as shown in Fig. 3 of Bond et al. (1999), resulting in warm SST events (lows in *N. pachyderma* (s) abundance) being tied to interstadials, stadials, and/or transitions. Here, these original picks (open squares) are tied to the proper corresponding features of the NGRIP ice core record (blue, bottom). Radiocarbon dates are updated to Marine09 (filled circles), with inclusion of additional Site 609 radiocarbon dates (open circles). All ages plotted relative to A.D. 2000 (b2k).

maximum counting error (MCE) of GICC05, which is "the accumulated error obtained by summing up the uncertain annual layers" and is regarded as roughly equivalent to 2σ range (Svensson et al., 2008) (Table 3). To prevent potential age reversals due to overlapping uncertainty, one radiocarbon date at 87.5 cmbsf and two NGRIP tie points at 191.5 and 364.5 cmbsf are excluded.

50 ensembles of 100,000 alternate age models are calculated. Maximum allowable sedimentation rate and maximum change in

Table 2
Site 609 original and revised Greenland ice core tie points.

609 depth (cm)	%*Nps*	GISP2 depth (m)	GISP2 age (ka BP 1950)	GISP2 event	NGRIP depth (m)	NGRIP age (ka b2k)	NGRIP event	NGRIP chronology
139.5	L	2076	29.03	T	1890.14	28.50	I	GICC05
191.5	L	2176	35.23	I	2008.60	35.45	I	GICC05
213.5	L	2230	38.32	I	2067.93	38.15	I	GICC05
248.5	L	2276.8*	41.21	T	2123.82	41.45	I	GICC05
261.5	L	2301.92*	42.486	I	2156.58	43.30	I	GICC05
285.5	L	2356.075*	45.283	I	2216.73	46.65	I	GICC05
347.5	P	2465.9807**	53.4973	I	2347.85	54.40	S	GICC05
346.5	L	2488	56.24	I	2394.54	57.80	I	GICC05
369.5	L	2502	57.76	T	2414.50	59.05	I	GICC05
385.5	L	2536	62.11	S	2463.40	63.95	I	ss09sea
405.5	L	2564	66.02	S	2507.37	69.60	I	ss09sea
420.5	L	2584	68.75	T	2534.94	72.25	I	ss09sea
445.5	T	2612	73.02	T	2579.85	76.50	T	ss09sea

The tie points to GISP2 used to produce the age model for Site 609 are shown at left (Bond et al., 1999). These data are presented graphically in Fig. 3 of Bond et al. (1999) but are not presented in table format as above. At right are our ties of the same depths in Site 609 to the NGRIP ice core. A 705-year shift to younger ages is required to align GICC05 and ss09sea time scales at 60 ka (Svensson et al., 2008). %*Nps* = percentage of *N. pachydema* (s) relative to total planktic foraminifers; GISP2/NGRIP Event = Greenland climate event; I = interstadial; S = stadial; P = relative peak in *Nps* abundance; L = relative low in *Nps* abundance; T = Greenland/*Nps* transition; * = interpolated point; ** Based on the MS/94 age model for GISP2, which assigned ages of 53.22 ka and 53.5 ka to 2464 m and 2466 m, respectively, a tie point to a depth of exactly 2465.98071428571 m in GISP2 is required to obtain the age of 53.4973 ka that was assigned by Bond et al. (1999) to 347.5 cm in Site 609.

Table 3
Site 609 revised age model.

Site 609 depth (cmbsf)	Age (ka b2k)	2σ range for model	Tie point type	Chronology
55	13.03	−0.24 + 0.28	^{14}C*	Marine09
73.5	14.49	−0.84 + 0.50	^{14}C *Nps*	Marine09
79.5	16.24	−0.56 + 0.82	^{14}C *Gb*	Marine09
84.5	17.79	−0.68 + 0.58	^{14}C *Nps*	Marine09
87.5	19.17	N/A	^{14}C *Nps*	Marine09
90.5	19.56	−0.24 + 0.18	^{14}C *Nps*	Marine09
98.5	20.18	−0.32 + 0.38	^{14}C *Nps*	Marine09
107.5	22.66	−0.66 + 0.22	^{14}C *Nps*	Marine09
110.5	23.90	−0.76 + 0.84	^{14}C *Nps*	Marine09
111.5	24.58	−0.56 + 0.76	^{14}C *Nps*	Marine09
112.5	25.28	−0.64 + 0.72	^{14}C *Nps*	Marine09
115.5	25.59	−0.70 + 0.62	^{14}C *Nps*	Marine09
118.5	27.05	−0.80 + 1.28	^{14}C *Nps*	Marine09
140.5	30.10	−0.94 + 0.76	^{14}C *Gi*	Marine09
148.5	30.89	−0.42 + 0.50	^{14}C *Nps*	Marine09
153.5	31.98	−1.20 + 1.82	^{14}C *Nps*	Marine09
166.5	33.20	−2.0 + 1.16	^{14}C *Nps*	Marine09
174.5	33.92	−1.34 + 0.60	^{14}C *Gi*	Marine09
191.5	35.45	N/A	% *Nps*	GICC05
213.5	38.15	±1.44	% *Nps*	GICC05
248.5	41.45	±1.64	% *Nps*	GICC05
261.5	43.30	±1.74	% *Nps*	GICC05
285.5	46.65	±1.90	% *Nps*	GICC05
347.5	54.40	±2.32	% *Nps*	GICC05
346.5	57.80	N/A	% *Nps*	GICC05
369.5	59.05	±2.56	% *Nps*	GICC05
385.5	63.95	–	% *Nps*	ss09sea
405.5	69.60	–	% *Nps*	ss09sea
420.5	72.25	–	% *Nps*	ss09sea
445.5	76.50	–	% *Nps*	ss09sea

Age control points used in the “best-fit” age model of (Fig. 2). The three oldest radiocarbon dates are adjusted within 2σ range, optimizing the fit to the NGRIP-correlated section. The tie point to NGRIP at 139.5 cm overlaps with the newly calibrated radiocarbon dates and is not used for the updated Site 609 age model. N/A refers to tie points excluded from the age uncertainty model, and ss09sea ages have no reported error range. *Nps* = *N. pachyderma* (s); *Gb* = *G. bulloides*; *Gi* = *G. inflata*. * ^{14}C date at 55 cm was performed on undisclosed material.

sedimentation rate are specified as 20 and 15 cm/k.y., respectively, which are approximately twice the values exhibited by the best-fit age model. Alternate age models that exceeded these parameters are discarded. Each of the accepted age models are applied to the Site 609 HSG series, which is then analyzed by multitaper method spectral analysis (MTM) after interpolation to a 200-year fixed time step. A distribution is populated from the frequencies of spectral peaks exhibiting at least 95% confidence relative to an AR(1) background. Results are reported as the mean and standard deviation of all 50 distributions.

The above results are then compared to results from synthetic series passed through the same age uncertainty model. These are designed to exhibit similar spectral characteristics as the Site 609 HSG series, which was best simulated by adding pink noise to sine waves based on frequencies identified during spectral analysis of the best-fit age model. Both single- and combined-frequency waves are used. Each series is then interpolated to the same age scale as the Site 609 HSG record. Finally, the first and second SSA-reconstructed HSG components are added in order to create a similar low-frequency, non-linear trend as the Site 609 HSG series (Fig. S2). Model convergence and stability are obtained with shorter runs of 20 ensembles of 10,000 alternate age models.

4. Results

4.1. Site 609 updated chronology

Several errors in the original site 609 correlation to the Greenland ice record are corrected. The Bond et al. (1999) ties to GISP2 are not optimal and vary in relative phasing, resulting in individual lows in *N. pachyderma* (s) abundance (relatively warm SST) being inconsistently tied to Greenland stadials, interstadials, or transitions.

The age model presented here for Site 609 (Table 3) is adjusted slightly to optimize the fit between the radiocarbon and ice core derived ages. The youngest Greenland ice core tie point of Bond et al. (1999), located at 139.5 cmbsf, is not required because it overlaps with the radiocarbon dated interval. In addition, without adjustment, the interval between the oldest radiocarbon date (174.5 cmbsf; 35.36 ± 0.73 ka) and the next youngest ice core tie point (191.5 cmbsf; 35.45 ka) produces an abrupt, two order of magnitude increase in sedimentation rate exceeding 400 cm/k.y. (Fig. 3a). Therefore, the three oldest radiocarbon dates are adjusted

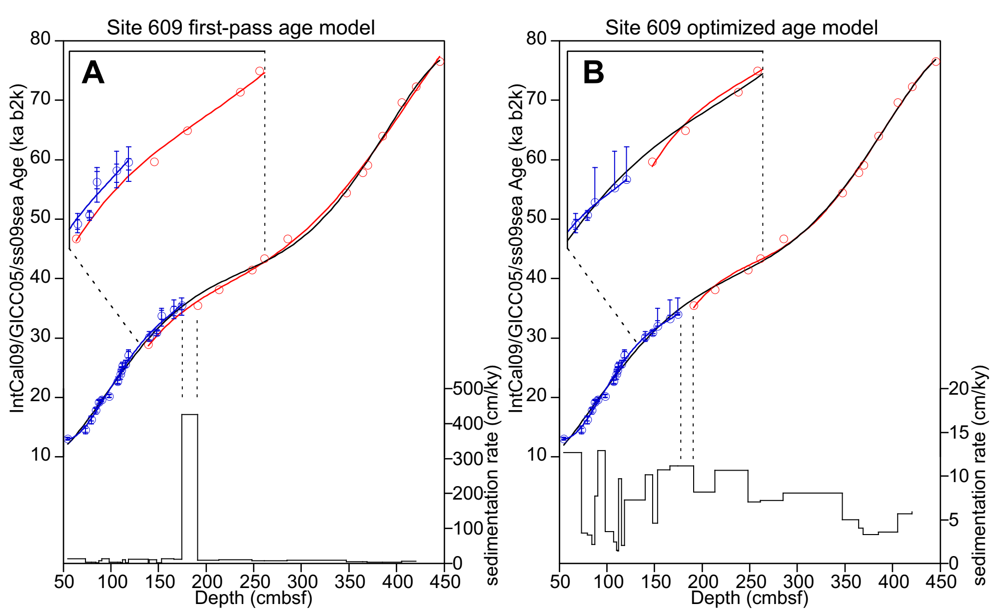

Fig. 3. A) Main panel shows sedimentation rate (black, bottom), the mean probability of Marine09 calibrated radiocarbon ages (blue circles) with associated 1σ and 2σ error ranges (inner and outer error bars) (Table 1), and NGRIP-derived ages (red circles) (Table 2). Upper inset shows offset between overlapping ice core tie points and radiocarbon ages. B) The three oldest radiocarbon dates are adjusted within 2σ range to produce a more reasonable sedimentation rate (Table 3). Solid lines show polynomial fit through age points.

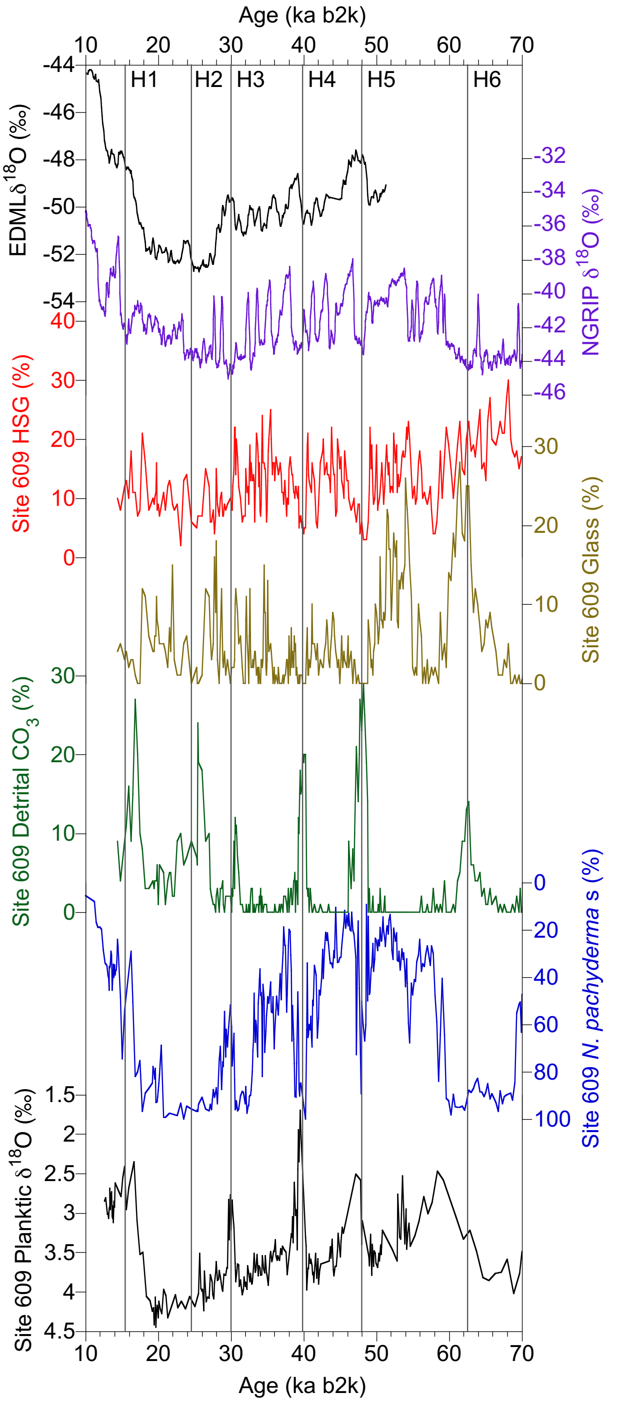

Fig. 4. Antarctic EDML (black) (EPICA Community Members, 2006) and Greenland NGRIP (purple) (NGRIP Project Members, 2004) ice core $\delta^{18}O$ records are plotted above Site 609 HSG (red), IG (brown), DC (green), % *N. pachyderma* (s) (blue), and *N. pachyderma* (s) $\delta^{18}O$ (black) (Bond et al., 1999). All records plotted on NGRIP GICC05 chronology.

within their 2σ range to produce a more reasonable sedimentation rate (Fig. 3b). Specifically, the radiocarbon dates at 153.5 and 166.5 cmbsf are adjusted to 31.98 and 33.20 ka, respectively, and an age of 33.92 ka is obtained for the oldest radiocarbon date at 174.5 cmbsf by linear interpolation between 33.20 ka and 35.45 ka, forcing no change in sedimentation rate. The updated chronology results in generally older ages for the Site 609 age model, with progressively increasing offset beginning from ∼40 ka and reaching a maximum of ∼4 k.y. by 70 ka (Fig. 2).

NGRIP and all available Site 609 data are plotted in our updated chronology with the Antarctic EDML ice core as a South Atlantic counterpart (Fig. 4). All series, including EDML, are plotted on the NGRIP GICC05 age scale (EPICA Community Members, 2006). Increases in IG and HSG coincide with reduced SST during Greenland stadials and precede peaks in DC and planktic $\delta^{18}O$, both of which indicate greatly increased discharge of LIS-derived icebergs (Bond and Lotti, 1995; Bond et al., 1999). Warming in Antarctica occurs subsequent to the onset of each of these “Hudson Strait” Heinrich Events (H1, H2, H4, and H5), as reduced production of North Atlantic Deep Water would result in diminished northward heat transport (Crowley, 1992).

4.2. Spectral analysis

Bond et al. (1999) reported an average elapsed time between Site 609 HSG cycle midpoints of 1476 ± 584 years but did not specify the down-core intervals defining each cycle. Our independent calculation of cycle midpoints results in an indistinguishable average length of 1492 ± 571 years with the original Bond chronology, and 1573 ± 669 years with our updated chronology. A number of spectral peaks are apparent at 1/2180, 1/1670, 1/1390, 1/980, 1/850, and 1/750 years (Fig. 5). While the 1/1390-year peak exhibits the highest amplitude relative to an AR(1) background, wavelet analysis indicates that it is nonstationary, and power in this band results primarily from the ss09sea-dated interval (>60 ka) that comprises the oldest 10 k.y. of the record (Fig. 6). The distribution of elapsed time between cycle midpoints in the GICC05-dated interval (<60 ka) exhibits two primary modes at ∼1000- and ∼2000-year wait-times (Fig. 7).

4.3. Alternate age models

Of the total 100,000 alternate age models calculated per each of the 50 ensembles, on average, 3612 ± 222 (1σ) are within the specified sedimentation rate criteria (Fig. 8). The ensemble-mean distribution of 95% confident significant spectral frequencies exhibits two primary bands. A 1/975 ± 50 year frequency is present in ∼45% of all age models (1587), and a relatively wide band centered at 1/2050 ± 150 years is detected in ∼20% (760). A third, minor band located at 1/1400 ± 30 years is significant in 12% (427) (Fig. 9).

Out of the five synthetic series created (Fig. S3), only two combined-frequency series produced results with significant correlation to results from the HSG series. The first series is constructed with equal amplitude 1/1025- and 1/2100-year frequencies ($r^2 = 0.83$), and the other adds a 1/1390-year frequency, with the 1/2100- and ∼1/1390-year components scaled respectively at 95% and 50% through iterative adjustment to maximize correlation ($r^2 = 0.86$) (Fig. 10).

5. Discussion

The absence of any identifiable external 1500-year forcing focused several efforts to explain such climate variability through ice-sheet modulation. Combination tones and heterodynes of centennial-scale cycles in inferred Holocene solar proxy records, such as directly observed sunspot cycles or atmospheric ^{14}C production, could be combined to produce frequencies consistent with those observed in many glacial records, including 1/1470 years (e.g., Braun et al., 2005; Clemens, 2005). However, all possible heterodynes of statistically significant frequencies in the IntCal09 ^{14}C production record are calculated to demonstrate that the millennial band (lower than and including 1/500 years) is saturated such that, by chance, any particular significant spectral peak from

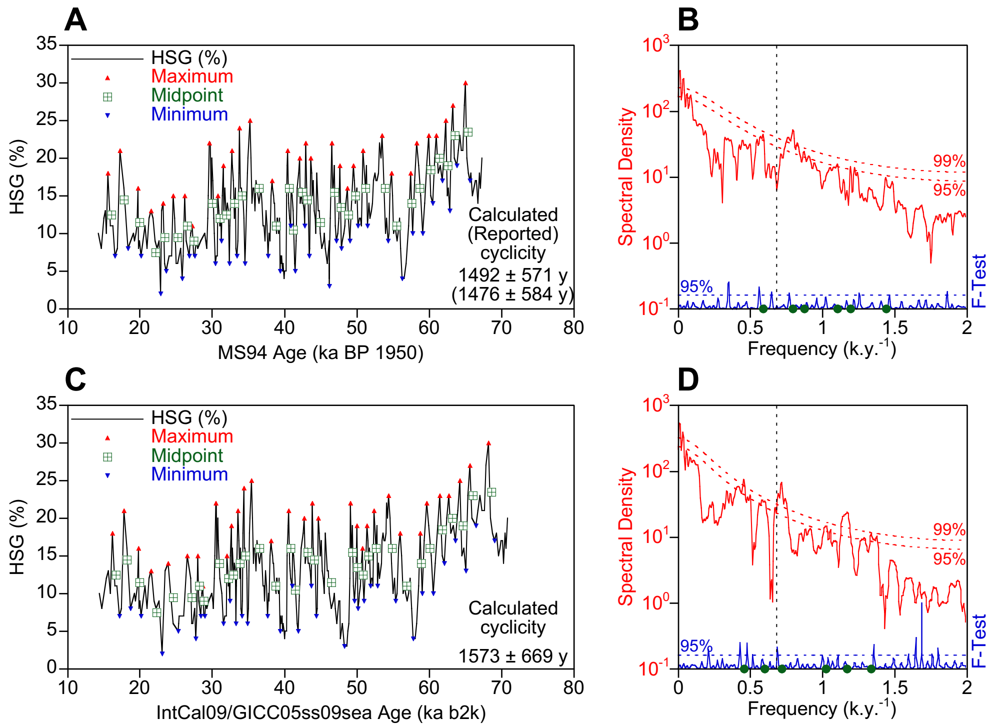

Fig. 5. A) Cycle midpoints for site 609 HSG using the Bond et al. (1999) age model were reported to produce 1476 ± 584 (we calculated 1492 ± 571) year cyclicity (midpoint to midpoint) but B) did not exhibit 1470-year spectral power. C) Site 609 HSG plotted with updated chronology contains a D) statistically significant (99% confidence) spectral peak at ~1/1390 years (1/1470–1/1330 year range). Upper and lower red dashed lines denote 99% and 95% confidence relative to an AR(1) background, respectively; blue dashed lines denote 95% confidence of periodicity by *F*-Test; and green dots indicate narrow-band, significant peaks relative to an AR(1) background. MTM power spectra calculated using the SSA-MTM toolkit (Ghil et al., 2002).

any particular climate record will appear to correspond to ^{14}C production (Fig. 11).

If the Site 609 HSG variability is indeed solar in origin, a more parsimonious explanation is that it is directly related to the observed variability in the inferred forcings, the ~1000- and ~2000-year periods that are present in both Holocene atmospheric ^{14}C production and ice core ^{10}Be flux (Fig. S4). This is consistent with both wavelet analysis (Fig. 6) and age uncertainty modeling (Fig. 7) results that indicate these components are strongly significant throughout glacial Stages 2 and 3. The lack of these oscillations during the extended warm periods of Greenland Interstadial 12 (~43–47 ka) and 13–14 (~50–55 ka) may reflect circulation changes similar to those proposed for the Holocene (Bond et al., 1997). The low late-glacial sedimentation rates at Site 609 (Fig. 3) preclude the detection of 1000-year periodicity from 15 to ~30 ka, which is indicated by the regions of Fig. 6 from which shading is removed.

Therefore, the “1500-year cycle” is more likely to be either an artifact of arithmetic averaging or the result of chronological uncertainty. Within the GICC05-dated interval (<60 ka) of Site 609,

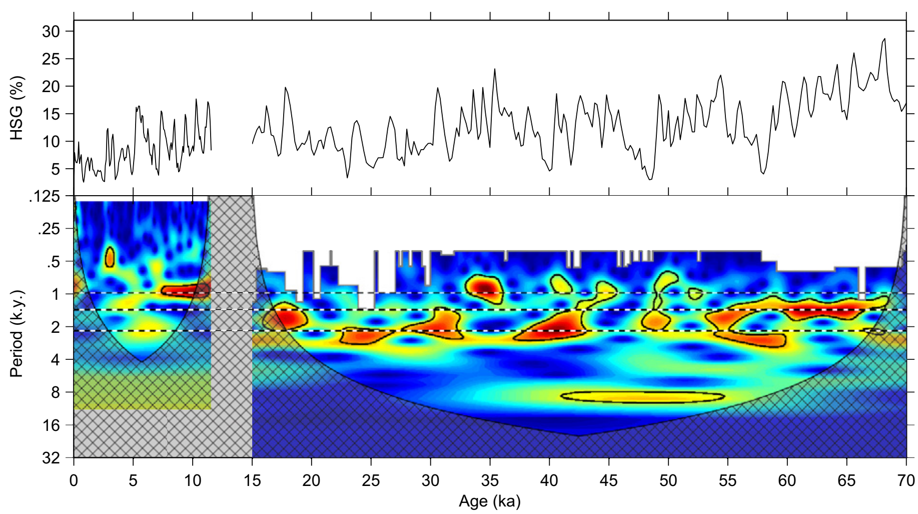

Fig. 6. Wavelet analysis of the stacked Holocene HSG record of Bond et al. (2001) (left) and DSDP Site 609 (Bond et al., 1999) (right). Solid black lines indicate the 95% confidence intervals, and the hatched area represents the cone of influence. The 609 record was interpolated to a 200-year time step, detrended, and filtered to removed frequencies higher than 500 years. White areas in the wavelet indicate the nyquist frequency of the Site 609 series prior to 200-year interpolation.

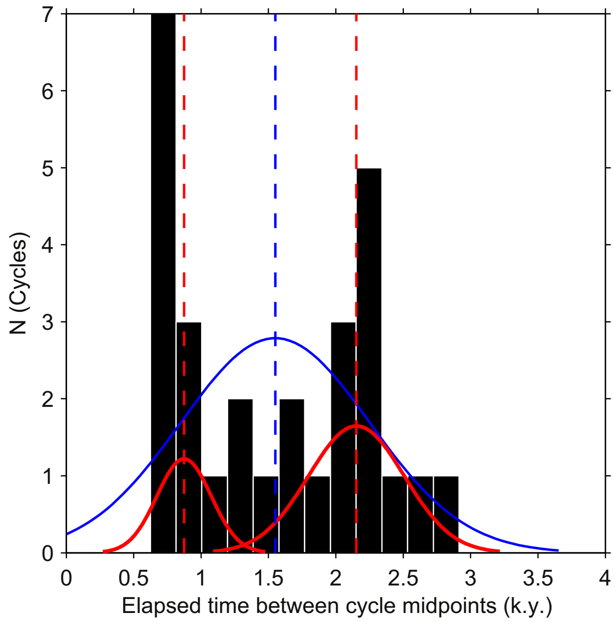

Fig. 7. Interval counting the elapsed time between cycle midpoints for the GICC05 interval of Site 609 results in a bimodal distribution. The two modes at ~1000 and ~2000 years average to 1500 years. Wide blue curve is a Gaussian fit to the entire distribution. Narrow red curves are fit to two distributions split at 1500 years.

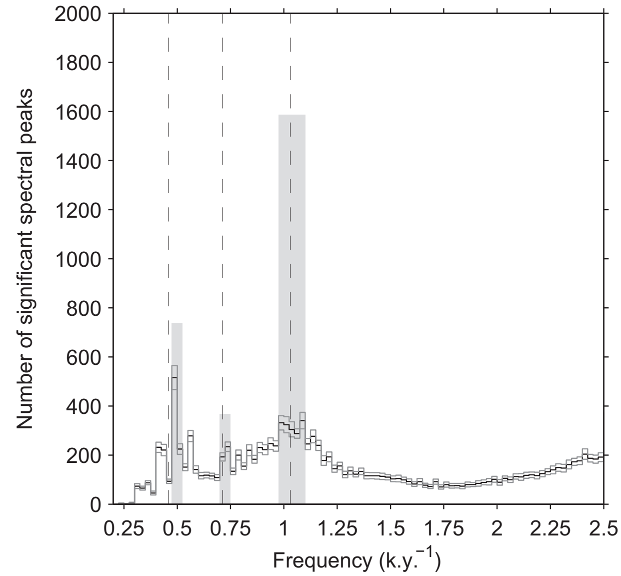

Fig. 9. Distribution of ensemble-mean and 1σ range of significant spectral peaks in alternate age models. Shaded vertical bars indicate sum total within each band. Vertical dashed lines indicate the frequency of millennial-scale spectral peaks in best-fit age model (1/2180, 1/1390, and 1/980 years). Results are plotted in the frequency domain, causing lower (higher) frequency bands to appear artificially narrow (wide) (See text for explanation of bandwidths).

the ~1500-year average cycle length corresponds to the non-existent mean in a bimodal distribution dominated by ~1000- and 2000-year wait times between HSG deposition events (Fig. 7). Considering the entire record, only 4 of the 34 HSG cycles resolved at Site 609 exhibit a length within 150 years of 1500. These are primarily limited to the oldest interval (>60 ka), corresponding to MIS 4, which exhibits the highest chronological uncertainty due the sole age constraint being the ss09sea ice flow model. As shown by wavelet analysis, this short interval contributes substantially to the relatively high amplitude of the ~1500-year spectral peak evident in MTM results (Fig. 5). There exists little 1500-year significant variance in the interval younger than 60 ka, either at Site 609 or within the stacked Holocene HSG record of Bond et al. (2001) (Fig. 6). If not the product of averaging or uncertainty, that the 1500-year periodicity is limited to MIS 4 could indicate unique ice sheet boundary conditions subsequent to glacial inception.

Furthermore, analysis of a synthetic series indicates that chronological uncertainty in the most well-constrained interval (<60 ka) of Site 609 is sufficiently large to produce 1500-year periodicity from ~1000- and 2000-year forcings. A simple series based on equal amplitude sine waves at the 1/1025- and 1/2100-year frequencies explains 83% of the variability in the Site 609 HSG series, and a small proportion of realizations contain 1500-year periodicity, even though no 1500-year forcing is specified (Fig. 10).

However, the results of chronological uncertainty modeling cannot entirely discount a 1500-year period. Therefore additional synthetic series are also considered. Though the highest correlation is obtained when a weak 1390-year component is included and

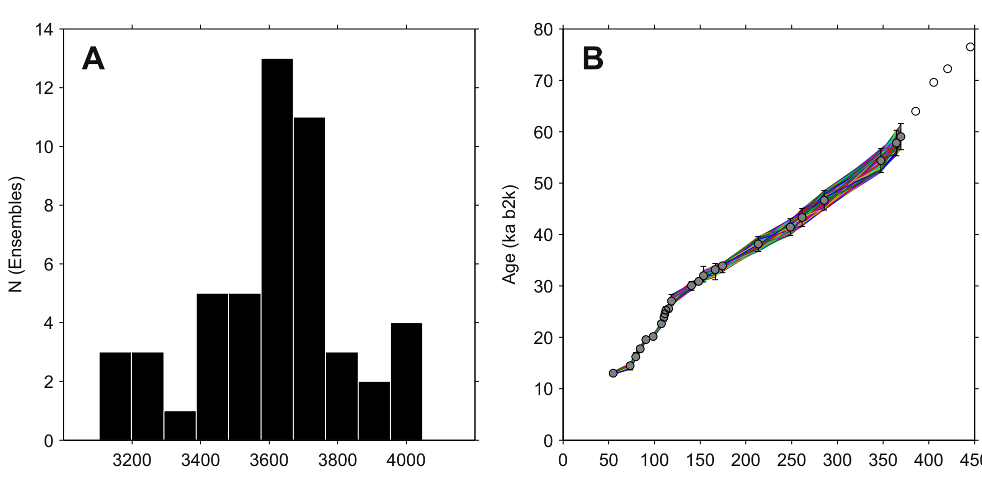

Fig. 8. A) Number of age models per ensemble that exhibit 1) less than a 20 cm/k.y. maximum sedimentation rate and 2) a maximum differential sedimentation rate of 15 cm/k.y. The total ranged from 4048 (ensemble 17) to 3104 (ensemble 45). B) All age–depth relationships ($N = 3348$) from a representative ensemble. Error bars denote 2σ age error. Unfilled circles indicate ages based on the ss09sea ice flow model, for which no published error exists.

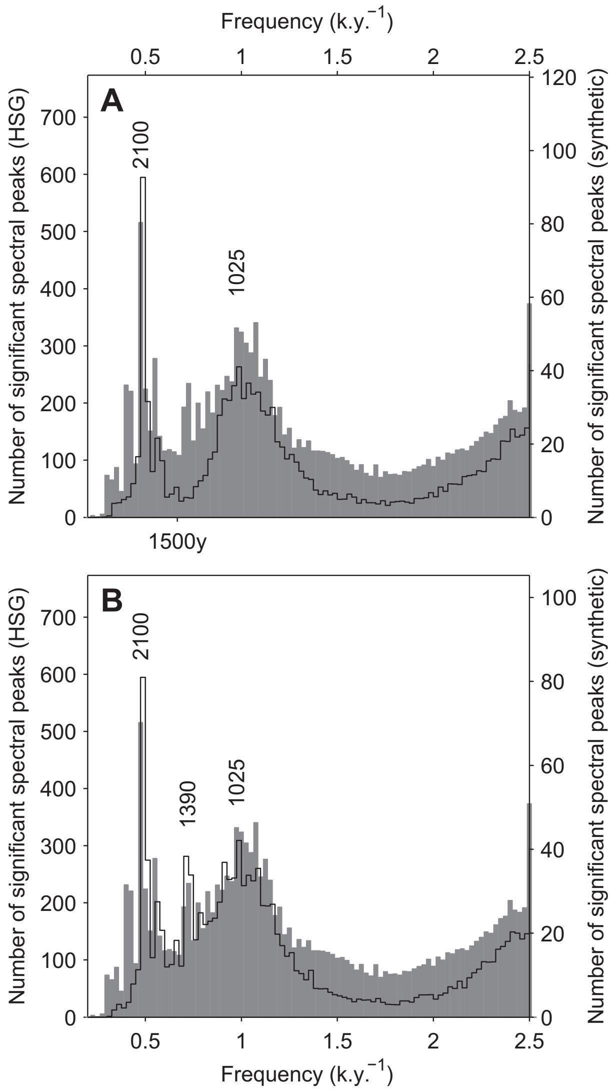

Fig. 10. Age uncertainty model results of HSG compared to A) age uncertainty model results from a series constructed from 1/2100- and 1/1025-year sine waves of equal amplitude. B) Model results with 1/2100 (95% amplitude), 1/1390 (50% amplitude), and 1/1025 (100% amplitude) sine waves.

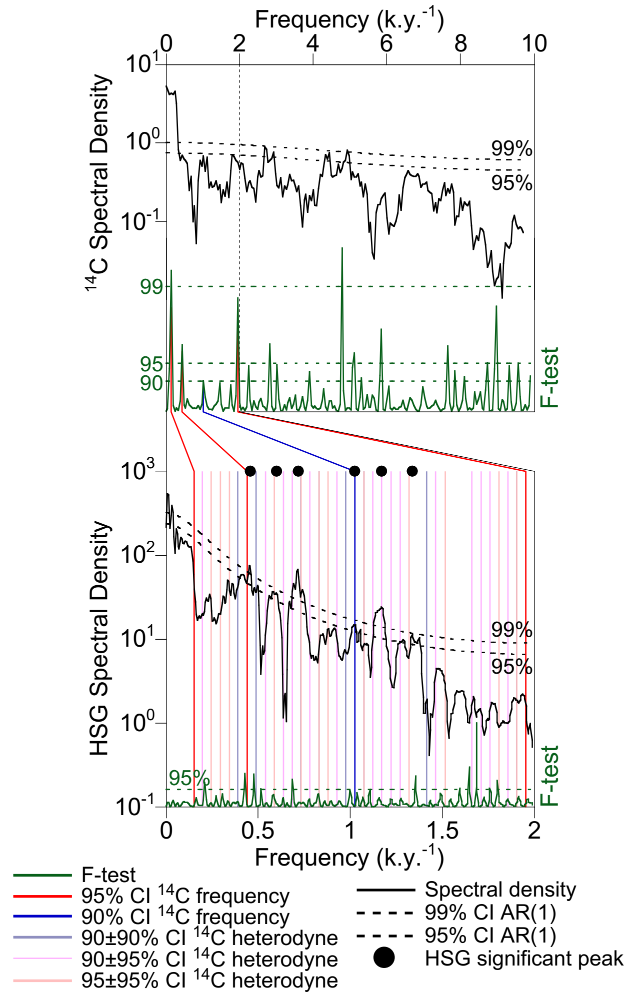

Fig. 11. MTM power spectrum with *F*-test (green) and confidence intervals for IntCal 09 ^{14}C production (analyzed to a 1/100 year frequency, top) and HSG (bottom). The frequencies of significant periods in ^{14}C production are shown as dark red and dark blue lines for 95% and 90% confidence respectively as determined by *F*-test. Light colored lines represent heterodynes of all >90% confident peaks in the production series to 1/100 years. Black circles indicate the location of discrete spectral peaks in the HSG series.

scaled such that it is at 50% amplitude relative to the 1/1025-year sine wave, this results in only a marginal improvement (r^2 increased from 0.83 to 0.86) at the cost of increased complexity. Inclusion of the third sine wave actually slightly diminishes the correlation in the millennial band, between 1/2100 and 1/900 years, from $r^2 = 0.81$ to 0.78. These observations also support primary HSG variability at ~1000- and 2000-year intervals.

While Debret et al. (2007) argued for late Holocene ~1500-year HSG periodicity in the stacked record of Bond et al. (2001), spectral power at this frequency neither passes a significance test at 95% confidence nor is free from record edge effects (Fig. 6). SSA results further indicate that a discrete 1500-year component is not present in the Holocene HSG stack, though the second principal component (PC2) oscillates at a nearby frequency (1750 years). Reconstructing the Holocene HSG stack with only seven components and specifically excluding PC2 (e.g., PC1, PC3-8) yields a series that describes 88% of the variability in the raw series, captures all major features in both the time and frequency domains, and remains consistent with the Bond et al. (2001) conclusions (Fig. S4).

In addition to the last glacial and Holocene HSG records, a ~1000-year period is also detected in a number of Holocene records (Sirocko et al., 1996; Campbell et al., 1998; deMenocal et al., 2000; Hu et al., 2003; Viau et al., 2006), including a composite Northern Hemisphere record of Alpine glacier fluctuations (Crowley, 2010) (Fig. S5). There are comparatively few Holocene records that exhibit 1500-year periodicity, with the primary exception being the sortable silt record of Bianchi and McCave (1999). While Holocene dating is well constrained, its short duration presents challenges for time series analysis (e.g., Wanner et al., 2008). Therefore, the well-dated, key records of the last glaciation may prove better suited for detection of millennial-scale periodicity.

Now that the 1470-year spectral peak in the GISP2 $\delta^{18}O$ record has been shown to be insignificant if not for three D-O Events (Schulz, 2002), absent in NGRIP (Ditlevsen et al., 2007), and, in the case of HSG, most likely an artifact of averaging with minimal statistical justification, relatively little support remains for actual 1500-year intervals of climate variability. Evidence does exist, however, for solar variations at periods of ~1000 and ~2000 years, though more work is required to separate the effects of geomagnetic field variability (St-Onge et al., 2003; Snowball and Muscheler, 2007). If these inferred solar cycles statistically exist, then conceivably higher climate sensitivity during the intermediate interval of global ice volume may explain the apparently larger millennial-scale fluctuations in MIS 3 than in the Holocene.

6. Conclusions

An updated chronology for classic DSDP Site 609 is based on the latest radiocarbon calibration (Marine09) and Greenland ice core chronology (GICC05). With this new age model, the hematite-stained grain (HSG) ice-rafting proxy, well known for displaying a "1500-year cycle," exhibits primary variability at 1000- and 2000-year periods. Thus, the original 1476 $\pm$ 585 year result reported for Site 609 (Bond et al., 1999) is likely an admixture of one longer and one shorter cycle. Chronological modeling indicates that a 1500-year component, if indeed present, would be relatively minor and potentially the result of age model uncertainty. Taking into account this uncertainty, the variability in HSG over the millennial frequency band is most consistent with dual 1000 and 2000-year forcing, similar to the variability in inferred solar proxies. Therefore, HSG provides relatively little data supporting actual 1500-year intervals of climate variability in either the Holocene or last glacial. The number is likely an artifact of averaging and seems to have little statistical justification.

Acknowledgments

The scientific contributions of G.C. Bond sparked much fruitful debate on the nature of millennial climate. Rusty Lotti-Bond provided the full dataset for Site 609, without which this work would not have been possible. We are also indebted to P.A. Baker, B.J. Corliss, and G.S. Dwyer. The work contained in this manuscript was conducted at the University of Tokyo Atmosphere and Ocean Research Institute (formerly the Ocean Research Institute) with funding from the JSPS (Kakenhi 23654080, 22101005, 22244061, 20.08826 and the NEXT program GR031). Post-expedition research funding was provided by JOI/USSSP.

Appendix A. Supplementary material

Supplementary data related to this article can be found online at http://dx.doi.org/10.1016/j.quascirev.2012.08.008.

References

Bard, E., Arnold, M., Fairbanks, R.G., Hamelin, B., 1993. ^{230}Th–^{324}U and ^{14}C ages obtained by mass spectrometry on coral. Radiocarbon 35 (1), 191–199.
Belt, E.S., 1965. Stratigraphy and paleogeography of Mabou Group and related Middle Carboniferous facies, Nova Scotia, Canada. Geological Society of America Bulletin 76 (7), 777–802.
Bender, M., Sowers, T., Dickson, M.-L., Orchardo, J., Grootes, P., Mayewski, P.A., Meese, D.A., 1994. Climate correlations between Greenland and Antarctica during the past 100,000 years. Nature 372 (6507), 663–666.
Bianchi, G.G., McCave, I.N., 1999. Holocene periodicity in North Atlantic climate and deep-ocean flow south of Iceland. Nature 397 (6719), 515–517.
Bond, G.C., Lotti, R., 1995. Iceberg discharges into the North-Atlantic on millennial time scales during the last glaciation. Science 267 (5200), 1005–1010.
Bond, G.C., Showers, W., Cheseby, M., Lotti, R., Almasi, P., deMenocal, P., Priore, P., Cullen, H., Hajdas, I., Bonani, G., 1997. A pervasive millennial-scale cycle in North Atlantic Holocene and glacial climates. Science 278 (5341), 1257–1266.
Bond, G.C., Showers, W., Elliot, M., Evans, M.N., Lotti, R., Hajdas, I., Bonani, G., Johnsen, S., 1999. The North Atlantic's 1–2 kyr climate rhythm: relation to Heinrich events, Dansgaard/Oeschger cycles and the little ice age. In: Clark, P.U., Webb, R.S., Keigwin, L.d. (Eds.), Mechanisms of Global Climate Change at Millennial Time Scales. AGU, Washington D.C., pp. 35–68.
Bond, G.C., Heinrich, H., Broecker, W., Labeyrie, L., McManus, J., Andrews, J., Huon, S., Jantschik, R., Clasen, S., Simet, C., Tedesco, K., Klas, M., Bonani, G., Ivy, S., 1992. Evidence for massive discharges of icebergs into the North-Atlantic ocean during the Last Glacial Period. Nature 360 (6401), 245–249.
Bond, G.C., Broecker, W., Johnsen, S., McManus, J., Labeyrie, L., Jouzel, J., Bonani, G., 1993. Correlations between climate records from North-Atlantic sediments and Greenland Ice. Nature 365 (6442), 143–147.
Bond, G.C., Kromer, B., Beer, J., Muscheler, R., Evans, M.N., Showers, W., Hoffmann, S., Lotti-Bond, R., Hajdas, I., Bonani, G., 2001. Persistent solar influence on North Atlantic climate during the Holocene. Science 294 (5549), 2130–2136.
Braun, H., Christl, M., Rahmstorf, S., Ganopolski, A., Mangini, A., Kubatzki, C., Roth, K., Kromer, B., 2005. Possible solar origin of the 1470-year glacial climate cycle demonstrated in a coupled model. Nature 438 (70695), 208–211.
Campbell, I.D., Campbell, C., Apps, M.J., Rutter, N.W., Bush, A.B.G., 1998. Late Holocene ~1500 yr climatic periodicities and their implications. Geology 26 (5), 471–473.
Clemens, S.C., 2005. Millennial-band climate spectrum resolved and linked to centennial-scale solar cycles. Quaternary Science Reviews 24 (5–6), 521–531.
Conolly, J.R., Needham, H.D., Heezen, B.C., 1967. Late Pleistocene and Holocene sedimentation in the Laurentian Channel. The Journal of Geology 75 (2), 131–147.
Crowley, T.J., 2010. Assessing the sun–climate relationship in paleoclimate records. In: Schrijver, C.J., Siscoe, G.L. (Eds.), Heliophysics: Evolving Solar Activity and the Climates of Space and Earth. Cambridge University Press, Cambridge.
Crowley, T.J., 1992. North Atlantic deep water cools the Southern Hemisphere. Paleoceanography 7 (4), 489–497.
Debret, M., Bout-Roumazeilles, V., Grousset, F., Desmet, M., McManus, J.F., Massei, N., Sebag, D., Petit, J.-R., Copard, Y., Trentesaux, A., 2007. The origin of the 1500-year climate cycles in Holocene North-Atlantic records. Climates of the Past 3 (4), 569–575.
deMenocal, P.B., Ortiz, J.D., Guilderson, T.P., Sarnthein, M., 2000. Coherent high- and low-latitude climate variability during the Holocene warm period. Science 288 (5474), 2198–2202.
Ditlevsen, P.D., Andersen, K.K., Svensson, A., 2007. The DO-climate events are probably noise induced: statistical investigation of the claimed 1470 years cycle. Climates of the Past 3 (1), 129–134.
Elliot, M., Labeyrie, L., Bond, G.C., Cortijo, E., Turon, J.-L., Tisnerat, N., Duplessy, J.-C., 1998. Millennial-scale iceberg discharges in the Irminger Basin during the last glacial period: relationship with the Heinrich Events and environmental settings. Paleoceanography 13 (5), 433–446.
EPICA Community Members, 2006. One-to-one coupling of glacial climate variability in Greenland and Antarctica. Nature 444 (7116), 195–198.
Ericson, D.B., Ewing, M., Wollin, G., Heezen, B.C., 1961. Atlantic deep-sea sediment cores. Geological Society of America Bulletin 72 (2), 193–286.
Exp 303 Scientists, 2006. Site U1308. Proceedings of the Integrated Ocean Drilling Program Volume 303/306.
Ghil, M., Allen, M.R., Dettinger, M.D., Ide, K., Kondrashov, D., Mann, M.E., Robertson, A.W., Saunders, A., Tian, Y., Varadi, F., Yiou, P., 2002. Advanced spectral methods for climatic time series. Reviews of Geophysics 40 (1). http://dx.doi.org/10.1029/2000RG000092.
Grootes, P.M., Stuvier, M., 1997. Oxygen 18/16 variability in Greenland snow and ice with 10^{-3}- to 10^{5}-year time resolution. Journal of Geophysical Research 102 (C12), 26455–66470.
Heezen, B.C., Drake, C.L., 1964. Grand banks slump. AAPG Bulletin 48 (2), 221–225.
Heezen, B.C., Hollister, C.D., Ruddiman, W.F., 1966. Shaping of the continental rise by deep geostrophic contour currents. Science 152 (3721), 502–508.
Hodell, D.A., Curtis, J.H., 2008. Oxygen and carbon isotopes of detrital carbonate in North Atlantic Heinrich Events. Marine Geology 256 (1–4), 30–35.
Hodell, D.A., Channell, J.E.T., Curtis, J.H., Romero, O.E., Röhl, U., 2008. Onset of "Hudson Strait" Heinrich events in the eastern North Atlantic at the end of the middle Pleistocene transition (~640 ka)? Paleoceanography 23. http://dx.doi.org/10.1029/2008PA001591.
Hollister, C.D., 1967. Sediment Distribution and Deep Circulation in the Western North Atlantic. Ph.D. thesis, Columbia Univesity, New York.
Hu, F.S., Kaufman, D., Yoneji, S., Nelson, D., Shemesh, A., Huang, Y., Tian, J., Bond, G., Clegg, B., Brown, T., 2003. Cyclic variation and solar forcing of Holocene climate in the Alaskan Subarctic. Science 301 (5641), 1890–1893.
Marlowe, J.I., 1968. Unconsolidated marine sediments in Baffin Bay. Journal of Sedimentary Petrology 38 (4), 1065–1078.
Meese, D.A., Gow, A.J., Alley, R.B., Zielinski, G.A., Grootes, P.M., Ram, M., Taylor, K.C., Mayewski, P.A., Bolzan, J.F., 1997. The Greenland Ice Sheet Project 2 depth-age scale: methods and results. Journal of Geophysical Research 102 (C12), 26,411–26,423.
Needham, H.D., Habib, D., Heezen, B.C., 1969. Upper carboniferous palynomorphs as a tracer of red sediment dispersal patterns in the Northwest Atlantic. The Journal of Geology 77 (1), 112–120.
NGRIP Project Members, 2004. High-resolution record of Northern Hemisphere climate extending into the last interglacial period. Nature 431 (7005), 147–151.
Rahmstorf, S., 2003. Timing of abrupt climate change: a precise clock. Geophysical Research Letters 30 (10). http://dx.doi.org/10.1029/2003GL017115.
Reimer, P.J., Baillie, M.G.L., Bard, E., Bayliss, A., Beck, J.W., Blackwell, P.G., BronkRamsey, C., Buck, C.E., Burr, G.S., Edwards, R.L., Friedrich, M., Grootes, P.M., Guilderson, T.P., Hajdas, I., Heaton, T.J., Hogg, A.G., Hughen, K.A., Kaiser, K.F., Kromer, B., McCormac, F.G., Manning, S.W., Reimer, R.W., Richards, D.A., Southon, J.R., Talamo, S., Turney, C.S.M., vanderPlicht, J., Weyhenmeyer, C.E., 2009. IntCal09 and Marine09 radiocarbon age calibration curves, 0–50,000 years cal BP. Radiocarbon 51 (4), 1111–1150.
Ruddiman, W.F., 1977. Late Quaternary deposition of ice-rafted sand in the subpolar North Atlantic (lat 40 degrees to 65 degrees N). Geological Society of America Bulletin 88 (12), 1813–1827.
Schulz, M., 2002. On the 1470-year pacing of Dansgaard–Oeschger warm events. Paleoceanography 17 (2). http://dx.doi.org/10.1029/2000PA000571.

Sirocko, F., Garbe-Schönberg, D., McIntyre, A., Molfino, B., 1996. Teleconnections between the subtropical monsoons and high-latitude climates during the last deglaciation. Science 272 (5261), 526–529.
Snowball, I., Muscheler, R., 2007. Palaeomagnetic intensity data: an Achilles heel of solar activity reconstructions. The Holocene 17 (6), 851–859.
St-Onge, G., Stoner, J.S., Hillaire-Marcel, C., 2003. Holocene paleomagnetic records from the St. Lawrence Estuary, eastern Canada: centennial- to millennial-scale geomagnetic modulation of cosmogenic isotopes. Earth and Planetary Science Letters 209 (1–2), 113–130.
Stuiver, M., Reimer, P.J., 1993. Extended ^{14}C data base and revised CALIB 3.0 ^{14}C age calibration program. Radiocarbon 35 (1), 215–230.
Svensson, A., Andersen, K.K., Bigler, M., Clausen, H.B., Dahl-Jensen, D., Davies, S.M., Johnsen, S.J., Muscheler, R., Rasmussen, S.O., Röthlisberger, R., Peder Steffensen, J., Vinther, B.M., 2006. The Greenland Ice Core Chronology 2005, 15–42 ka. Part 2: comparison to other records. Quaternary Science Reviews 25 (23–24), 3258–3267.
Svensson, A., Andersen, K.K., Bigler, M., Clausen, H.B., Dahl-Jensen, D., Davies, S.M., Johnsen, S.J., Muscheler, R., Parrenin, F., Rasmussen, S.O., Röthlisberger, R., Seierstad, I., Steffensen, J.P., Vinther, B.M., 2008. A 60 000 year Greenland stratigraphic ice core chronology. Climate of the Past 4 (1), 47–57.
Torrence, C., Compo, G.P., 1998. A practical guide to wavelet analysis. Bulletin of the American Meteorological Society 79 (1), 61–78.
Viau, A.E., Gajewski, K., Sawada, M.C., Fines, P., 2006. Millennial-scale temperature variations in North America during the Holocene. Journal of Geophysical Research 111. http://dx.doi.org/10.1029/2005JD006031.
Wanner, H., Beer, J., Bütikofer, J., Crowley, T.J., Cubasch, U., Flückiger, J., Goosse, H., Grosjean, M., Joos, F., Kaplan, J.O., Küttel, M., Müller, S.A., Prentice, I.C., Solomina, O., Stocker, T.F., Tarasov, P., Wagner, M., Widmann, M., 2008. Mid- to Late Holocene climate change: an overview. Quaternary Science Reviews 27 (19–20), 1791–1828.
Zimmerman, H.B., 1972. Sediments of the New England continental rise. Geological Society of America Bulletin 83 (12), 3709–3724.